Search for new physics in $e^{\pm}q$ contact interactions at HERA

H1 Collaboration

C. Adloff [ag], V. Andreev [x], B. Andrieu [aa], T. Anthonis [d], A. Astvatsatourov [ai],
A. Babaev [w], J. Bähr [ai], P. Baranov [x], E. Barrelet [ab], W. Bartel [j], S. Baumgartner [aj],
J. Becker [ak], M. Beckingham [u], A. Beglarian [ah], O. Behnke [m], A. Belousov [x],
Ch. Berger [a], T. Berndt [n], J.C. Bizot [z], J. Böhme [j], V. Boudry [aa], W. Braunschweig [a],
V. Brisson [z], H.-B. Bröker [b], D.P. Brown [j], D. Bruncko [p], F.W. Büsser [k],
A. Bunyatyan [l,ah], A. Burrage [r], G. Buschhorn [y], L. Bystritskaya [w], A.J. Campbell [j],
S. Caron [a], F. Cassol-Brunner [v], V. Chekelian [y], D. Clarke [e], C. Collard [d],
J.G. Contreras [g,4], Y.R. Coppens [c], J.A. Coughlan [e], M.-C. Cousinou [v], B.E. Cox [u],
G. Cozzika [i], J. Cvach [ac], J.B. Dainton [r], W.D. Dau [o], K. Daum [ag,2], M. Davidsson [t],
B. Delcourt [z], N. Delerue [v], R. Demirchyan [ah], A. De Roeck [j,6], E.A. De Wolf [d],
C. Diaconu [v], J. Dingfelder [m], P. Dixon [s], V. Dodonov [l], J.D. Dowell [c], A. Droutskoi [w],
A. Dubak [y], C. Duprel [b], G. Eckerlin [j], D. Eckstein [ai], V. Efremenko [w], S. Egli [af],
R. Eichler [af], F. Eisele [m], E. Eisenhandler [s], M. Ellerbrock [m], E. Elsen [j], M. Erdmann [j,13,3],
W. Erdmann [aj], P.J.W. Faulkner [c], L. Favart [d], A. Fedotov [w], R. Felst [j], J. Ferencei [j],
S. Ferron [aa], M. Fleischer [j], P. Fleischmann [j], Y.H. Fleming [c], G. Flügge [b], A. Fomenko [x],
I. Foresti [ak], J. Formánek [ad], G. Franke [j], G. Frising [a], E. Gabathuler [r], K. Gabathuler [af],
J. Garvey [c], J. Gassner [af], J. Gayler [j], R. Gerhards [j], C. Gerlich [m], S. Ghazaryan [d,ah],
L. Goerlich [f], N. Gogitidze [x], C. Grab [aj], V. Grabski [ah], H. Grässler [b], T. Greenshaw [r],
G. Grindhammer [y], T. Hadig [m], D. Haidt [j], L. Hajduk [f], J. Haller [m], W.J. Haynes [e],
B. Heinemann [r], G. Heinzelmann [k], R.C.W. Henderson [q], S. Hengstmann [ak],
H. Henschel [ai], R. Heremans [d], G. Herrera [g,7], I. Herynek [ac], M. Hildebrandt [ak],
M. Hilgers [aj], K.H. Hiller [ai], J. Hladký [ac], P. Höting [b], D. Hoffmann [v], R. Horisberger [af],
A. Hovhannisyan [ah], S. Hurling [j], M. Ibbotson [u], Ç. İşsever [g], M. Jacquet [z], M. Jaffre [z],
L. Janauschek [y], X. Janssen [d], V. Jemanov [k], L. Jönsson [t], C. Johnson [c], D.P. Johnson [d],
M.A.S. Jones [r], H. Jung [t,j], D. Kant [s], M. Kapichine [h], M. Karlsson [t], O. Karschnick [k],
J. Katzy [j], F. Keil [n], N. Keller [ak], J. Kennedy [r], I.R. Kenyon [c], C. Kiesling [y], P. Kjellberg [t],
M. Klein [ai], C. Kleinwort [j], T. Kluge [a], G. Knies [j], A. Knutsson [t], B. Koblitz [y],
S.D. Kolya [u], V. Korbel [j], P. Kostka [ai], S.K. Kotelnikov [x], R. Koutouev [l], A. Koutov [h],
J. Kroseberg [ak], K. Krüger [j], T. Kuhr [k], D. Lamb [c], M.P.J. Landon [s], W. Lange [ai],

T. Laštovička [ai,ad], P. Laycock [r], E. Lebailly [z], A. Lebedev [x], B. Leißner [a], R. Lemrani [j],
V. Lendermann [j], S. Levonian [j], B. List [aj], E. Lobodzinska [j,f], B. Lobodzinski [f,j],
A. Loginov [w], N. Loktionova [x], V. Lubimov [w], S. Lüders [ak], D. Lüke [g,j], L. Lytkin [l],
N. Malden [u], E. Malinovski [x], S. Mangano [aj], R. Maraček [y], P. Marage [d], J. Marks [m],
R. Marshall [u], H.-U. Martyn [a], J. Martyniak [f], S.J. Maxfield [r], D. Meer [aj], A. Mehta [r],
K. Meier [n], A.B. Meyer [k], H. Meyer [ag], J. Meyer [j], S. Michine [x], S. Mikocki [f],
D. Milstead [r], S. Mohrdieck [k], M.N. Mondragon [g], F. Moreau [aa], A. Morozov [h],
J.V. Morris [e], K. Müller [ak], P. Murín [p,5], V. Nagovizin [w], B. Naroska [k], J. Naumann [g],
Th. Naumann [ai], P.R. Newman [c], F. Niebergall [k], C. Niebuhr [j], O. Nix [n], G. Nowak [f],
M. Nozicka [ad], J.E. Olsson [j], D. Ozerov [w], V. Panassik [h], C. Pascaud [z], G.D. Patel [r],
M. Peez [v], E. Perez [i], A. Petrukhin [ai], J.P. Phillips [r], D. Pitzl [j], R. Pöschl [z],
I. Potachnikova [l], B. Povh [l], J. Rauschenberger [k], P. Reimer [ac], B. Reisert [y], C. Risler [y],
E. Rizvi [c], P. Robmann [ak], R. Roosen [d], A. Rostovtsev [w], S. Rusakov [x], K. Rybicki [f,8],
D.P.C. Sankey [e], S. Schätzel [m], J. Scheins [j], F.-P. Schilling [j], P. Schleper [j], D. Schmidt [ag],
D. Schmidt [j], S. Schmidt [y], S. Schmitt [j], M. Schneider [v], L. Schoeffel [i], A. Schöning [aj],
T. Schörner-Sadenius [y], V. Schröder [j], H.-C. Schultz-Coulon [g], C. Schwanenberger [j],
K. Sedlák [ac], F. Sefkow [ak], I. Sheviakov [x], L.N. Shtarkov [x], Y. Sirois [aa], T. Sloan [q],
P. Smirnov [x], Y. Soloviev [x], D. South [u], V. Spaskov [h], A. Specka [aa], H. Spitzer [k],
R. Stamen [g], B. Stella [ae], J. Stiewe [n], I. Strauch [j], U. Straumann [ak], S. Tchetchelnitski [w],
G. Thompson [s], P.D. Thompson [c], F. Tomasz [n], D. Traynor [s], P. Truöl [ak], G. Tsipolitis [j,1],
I. Tsurin [ai], J. Turnau [f], J.E. Turney [s], E. Tzamariudaki [y], A. Uraev [w], M. Urban [ak],
A. Usik [x], S. Valkár [ad], A. Valkárová [ad], C. Vallée [v], P. Van Mechelen [d], A. Vargas
Trevino [g], S. Vassiliev [h], Y. Vazdik [x], A. Vest [a], A. Vichnevski [h], K. Wacker [g], J. Wagner [j],
R. Wallny [ak], B. Waugh [u], G. Weber [k], D. Wegener [g], C. Werner [m], N. Werner [ak],
M. Wessels [a], G. White [q], S. Wiesand [ag], T. Wilksen [j], M. Winde [ai], G.-G. Winter [j],
Ch. Wissing [g], M. Wobisch [j], E.-E. Woehrling [c], E. Wünsch [j], A.C. Wyatt [u], J. Žáček [ad],
J. Zálešák [ad], Z. Zhang [z], A. Zhokin [w], F. Zomer [z], M. zur Nedden [y]

[a] *I. Physikalisches Institut der RWTH, Aachen, Germany* [9]
[b] *III. Physikalisches Institut der RWTH, Aachen, Germany* [9]
[c] *School of Physics and Space Research, University of Birmingham, Birmingham, UK* [10]
[d] *Inter-University Institute for High Energies ULB-VUB, Brussels; Universiteit Antwerpen (UIA), Antwerpen, Belgium* [11]
[e] *Rutherford Appleton Laboratory, Chilton, Didcot, UK* [10]
[f] *Institute for Nuclear Physics, Cracow, Poland* [12]
[g] *Institut für Physik, Universität Dortmund, Dortmund, Germany* [9]
[h] *Joint Institute for Nuclear Research, Dubna, Russia*
[i] *CEA, DSM/DAPNIA, CE-Saclay, Gif-sur-Yvette, France*
[j] *DESY, Hamburg, Germany*
[k] *Institut für Experimentalphysik, Universität Hamburg, Hamburg, Germany* [9]
[l] *Max-Planck-Institut für Kernphysik, Heidelberg, Germany*
[m] *Physikalisches Institut, Universität Heidelberg, Heidelberg, Germany* [9]
[n] *Kirchhoff-Institut für Physik, Universität Heidelberg, Heidelberg, Germany* [9]

[o] *Institut für Experimentelle und Angewandte Physik, Universität Kiel, Kiel, Germany*

[p] *Institute of Experimental Physics, Slovak Academy of Sciences, Košice, Slovak Republic* [13,14]

[q] *School of Physics and Chemistry, University of Lancaster, Lancaster, UK* [10]

[r] *Department of Physics, University of Liverpool, Liverpool, UK* [10]

[s] *Queen Mary and Westfield College, London, UK* [10]

[t] *Physics Department, University of Lund, Lund, Sweden* [15]

[u] *Physics Department, University of Manchester, Manchester, UK* [10]

[v] *CPPM, CNRS/IN2P3, Univ. Mediterranee, Marseille, France*

[w] *Institute for Theoretical and Experimental Physics, Moscow, Russia* [19]

[x] *Lebedev Physical Institute, Moscow, Russia* [13]

[y] *Max-Planck-Institut für Physik, München, Germany*

[z] *LAL, Université de Paris-Sud, IN2P3-CNRS, Orsay, France*

[aa] *LPNHE, Ecole Polytechnique, IN2P3-CNRS, Palaiseau, France*

[ab] *LPNHE, Universités Paris VI et VII, IN2P3-CNRS, Paris, France*

[ac] *Institute of Physics, Academy of Sciences of the Czech Republic, Praha, Czech Republic* [13,16]

[ad] *Faculty of Mathematics and Physics, Charles University, Praha, Czech Republic* [13,16]

[ae] *Dipartimento di Fisica Università di Roma Tre and INFN Roma 3, Roma, Italy*

[af] *Paul Scherrer Institut, Villigen, Switzerland*

[ag] *Fachbereich Physik, Bergische Universität Gesamthochschule Wuppertal, Wuppertal, Germany*

[ah] *Yerevan Physics Institute, Yerevan, Armenia*

[ai] *DESY, Zeuthen, Germany*

[aj] *Institut für Teilchenphysik, ETH, Zürich, Switzerland* [17]

[ak] *Physik-Institut der Universität Zürich, Zürich, Switzerland* [17]

Editor: W.-D. Schlatter

Abstract

Deep-inelastic $e^{\pm}p$ scattering at high squared momentum transfer Q^2 up to $30\,000$ GeV^2 is used to search for eq contact interactions associated to scales far beyond the HERA centre of mass energy. The neutral current cross section measurements $d\sigma/dQ^2$, corresponding to integrated luminosities of 16.4 pb^{-1} of e^-p data and 100.8 pb^{-1} of e^+p data, are well described by the Standard Model and are analysed to set constraints on new phenomena. For conventional contact interactions lower limits are set on compositeness scales Λ ranging between 1.6–5.5 TeV. Couplings and masses of leptoquarks and squarks in R-parity violating supersymmetry are constrained to $M/\lambda > 0.3$–1.4 TeV. A search for low scale quantum gravity effects in models with large extra dimensions provides limits on the effective Planck scale of $M_S > 0.8$ TeV. A form factor analysis yields a bound on the radius of light quarks of $R_q < 1.0 \times 10^{-18}$ m.

© 2003 Published by Elsevier B.V.

1. Introduction

Deep inelastic neutral current scattering $ep \to eX$ at very high squared momentum transfer Q^2 allows one to study the structure of eq interactions at short distances and to search for new phenomena beyond the Standard Model (SM). The concept of four-fermion contact interactions (CI) provides a convenient method to investigate the interference of any new particle field associated to large scales with the γ and Z fields of the Standard Model. This Letter considers conventional contact interactions, such as general models of compositeness and the exchange of heavy leptoquarks and supersymmetric quarks, as well as low scale quantum gravity effects, which may be mediated via gravitons coupling to Standard Model particles and propagating into large extra spatial dimensions.

The present analysis is a continuation of previous studies [1] based on e^+p data [2]. New H1 cross section data on e^-p scattering [3] and on e^+p scattering data [4] lead to a substantially higher sensitivity to new physics phenomena. Similar studies of eq contact interactions have been performed by other experiments at HERA [5], LEP [6] and TEVATRON [7], providing results comparable to those presented here.

2. Data and analysis method

The data have been collected with the H1 detector at HERA and correspond altogether to an integrated luminosity of $\mathcal{L}_{\text{int}} = 117.2$ pb^{-1}. They consist of three data sets of different lepton charge and centre of mass energy $\sqrt{s}$ (see Table 1). The cross section measurements $d\sigma/dQ^2$ extend over a large range

Table 1

Reaction	$\mathcal{L}_{\text{int}}$ (pb^{-1})	$\sqrt{s}$ (GeV)	Run period	Ref.
$e^+p \to e^+X$	35.6 ± 0.53	301	1994–1997	[2]
$e^-p \to e^-X$	16.4 ± 0.3	319	1998–1999	[3]
$e^+p \to e^+X$	65.2 ± 0.95	319	1999–2000	[4]

of squared momentum transfers 200 GeV$^2 < Q^2 <$ 30000 GeV^2 for inelasticity $y < 0.9$. Details can be found in the quoted references. In this Letter a contact interaction analysis is presented for each of the two recent data sets and the combined data including the previous measurements.

The phenomenological models under study and the analysis method are described in more detail in Ref. [1]. The analysis investigates the measured cross sections $d\sigma/dQ^2$ and performs quantitative tests of the SM or CI models, applying a minimisation of the χ^2 function

$$\chi^2 = \sum_i \left(\frac{\hat{\sigma}_i^{\text{exp}} - \hat{\sigma}_i^{\text{th}}(1 - \sum_k \Delta_{ik}(\varepsilon_k))}{\Delta\hat{\sigma}_i} \right)^2 + \sum_k \varepsilon_k^2. \tag{1}$$

Here $\hat{\sigma}_i^{\text{exp}}$ and $\hat{\sigma}_i^{\text{th}}$ are the experimental and theoretical cross sections for the measurement point i and $\Delta\hat{\sigma}_i$ is the corresponding error including statistical and uncorrelated systematic errors added in quadrature. The functions $\Delta_{ik}(\varepsilon_k)$ describe correlated systematic errors for point i associated to a source k. They depend on the fit parameters ε_k, which are effectively pulls caused by systematics. In general the influence of the correlated systematic errors is small. The following dominant sources of correlations are included: an overall normalisation uncertainty of 1.5–1.8% de-
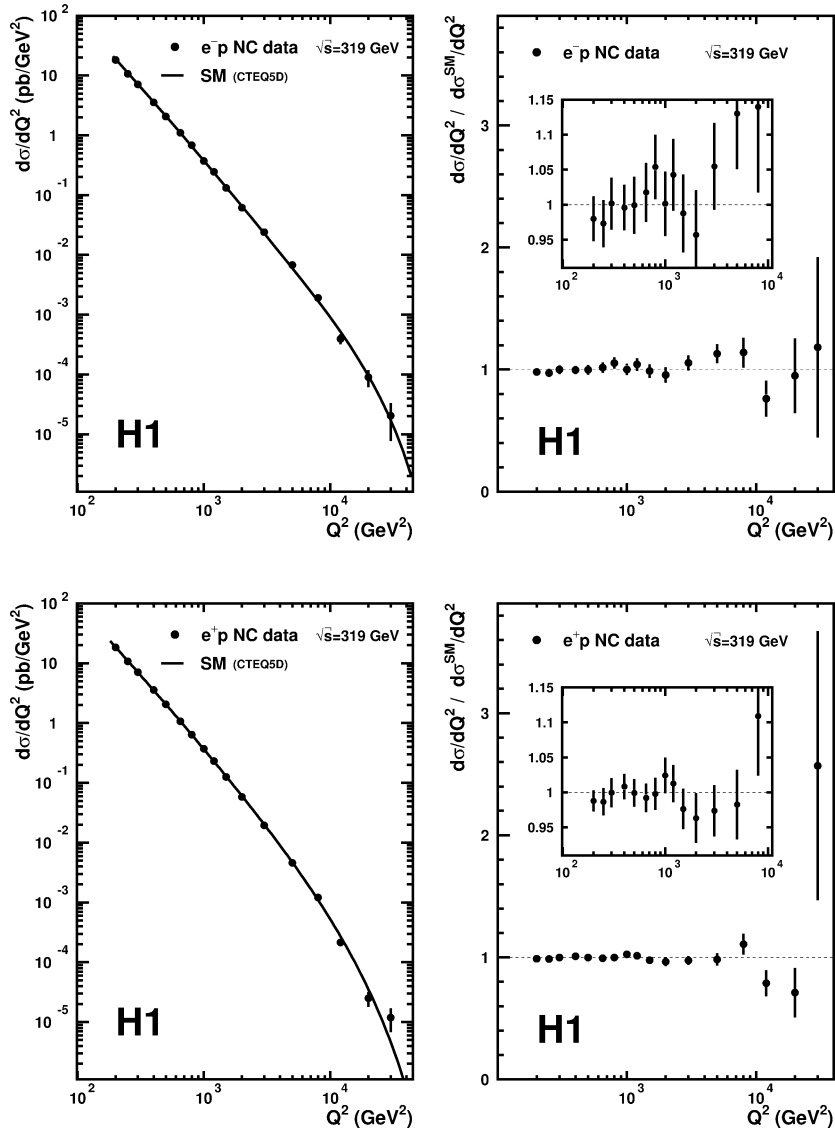
Fig. 1. Cross sections $d\sigma/dQ^2$ at $\sqrt{s} = 319$ GeV for $e^- p \rightarrow e^- X$ scattering (top) and $e^+ p \rightarrow e^+ X$ scattering (bottom). H1 data are compared with Standard Model expectations using the CTEQ5D parton distributions. The errors include only statistics and uncorrelated experimental systematics. Normalisation uncertainties are 1.8% ($e^- p$ data) and 1.5% ($e^+ p$ data).

pending on the run period, experimental uncertainties on the scattered lepton energy and angle and an uncertainty on the strong coupling $\alpha_s(M_Z) = 0.118 \pm 0.003$ entering the SM prediction. In a combined χ^2 analysis using Eq. (1) all data sets are treated as independent samples with individual normalisation and measurement uncertainties. The influence on the fit results of correlations between data sets is negligible.

The cross sections $d\sigma(e^- p \rightarrow e^- X)/dQ^2$ [3] and $d\sigma(e^+ p \rightarrow e^+ X)/dQ^2$ [4] from the new data are shown in Fig. 1.[1] They are very well described by the Standard Model expectations over the full Q^2 range,

---

[1] Corresponding figures for the $e^+ p$ cross sections at $\sqrt{s} = 301$ GeV [2] are shown in [1].

over which they vary by six orders of magnitude. Cross section calculations in the Standard Model are performed in the DIS scheme in next-to-leading order (NLO) QCD using the corresponding CTEQ5D parton parametrisation [8]. These parton distributions were obtained including the small amount of 2.7 pb^{-1} of 1994 H1 data with $Q^2 < 5000\,\text{GeV}^2$ only and are thus essentially uncorrelated with the present data.

Fits to the SM prediction yield $\chi^2 = 10.4$ for 17 degrees of freedom (dof) with a fitted normalisation of 0.998 for the $e^- p$ data and $\chi^2/\text{dof} = 13.9/17$ with a normalisation of 1.006 for the $e^+ p$ data, using statistical errors from the experiment and including all systematics as in Eq. (1). Applying other parton density functions like CTEQ6 [9], MRST [10] or GRV [11] leads to slight changes of the normalisation within errors, but yields equally good agreement with the data.

The cross section measurements do not show significant deviations from the Standard Model and will be used to set limits on couplings from processes mediated through contact interactions. Since the concept of contact interactions is an effective theory, theoretical expectations cannot be formulated consistently in NLO. A sensible approach is to reweight at each Q^2 value the SM NLO cross section by $\hat{\sigma}_i^{\text{LO}}(\text{SM} + \text{CI})/\hat{\sigma}_i^{\text{LO}}(\text{SM})$, the ratio of leading order (LO) cross sections with and without inclusion of contact interactions. The χ^2 function of Eq. (1) can be applied to evaluate the sensitivity of the data to a certain CI scenario and to determine its parameters. The corresponding limits at 95% confidence level (CL) are derived by using a frequentist approach as described in the appendix. Systematic uncertainties are included in this procedure. This determination of limits is different from the method used in our previous publication [1].

3. Contact interaction formalism

The most general chiral invariant Lagrangian for neutral current vector-like four-fermion contact interactions can be written in the form [12,13]

$$\mathcal{L}_V = \sum_q \sum_{a,b=L,R} \eta_{ab}^q (\bar{e}_a \gamma_\mu e_a)(\bar{q}_b \gamma^\mu q_b). \qquad (2)$$

For lepton e and each *up-type* and *down-type* quark flavour q with the corresponding currents e_a and q_b

there are four coupling coefficients $\eta_{ab}^q = \epsilon_{ab}(g/\Lambda_{ab}^q)^2$, where a and b indicate the L (left-handed) and R (right-handed) fermion helicities, g is the overall coupling strength, Λ_{ab}^q is a scale parameter and ϵ_{ab} determines the interference sign with respect to the Standard Model currents. Any particular model, such as compositeness or the exchange of leptoquarks or supersymmetric quarks, can be constructed by an appropriate choice of the couplings η_{ab}^q. The phenomenological models of interest and their analytical treatment are discussed in more detail in [1].

4. Compositeness scales

In general models allowing for fermion compositeness or substructure it is convenient to choose a coupling strength of $g^2 = 4\pi$ and to assume a universal scale Λ for all quarks. The contact interaction coefficients then read

$$\eta_{ab}^q = \epsilon_{ab} \frac{4\pi}{\Lambda^2}.$$

Various scenarios of chiral structures, e.g., pure L(eft) and R(ight) or V(ector) and A(xial vector) couplings, are defined by setting particular chiral contributions to values of $\epsilon_{ab} = \pm 1$ and setting all other combinations to zero.

The sensitivity to CI models is tested by determining the quantities ϵ/Λ^2 in a χ^2 fit using the experimental statistical and systematic errors and leaving the sign of interference free. The results from a combined fit to all data sets are shown in Fig. 2. The data tend to prefer negative interference, which may be due to some downward fluctuations at higher Q^2, but are consistent with the Standard Model within two standard deviations in all scenarios.

Lower limits on compositeness scale parameters $\Lambda^\pm$, associated to positive or negative interference, are derived from a frequentist approach and are summarised in Table 2. Despite the lower integrated luminosity, the $e^- p$ data exhibit for some models comparable (LL and RR couplings) or even higher (AA^+ coupling) sensitivity than the $e^+ p$ data. The two lepton charges complement each other and a combined analysis of all $e^\pm p$ data sets yields substantial improvements in most scenarios compared with the previous publication [1]. The results are presented in
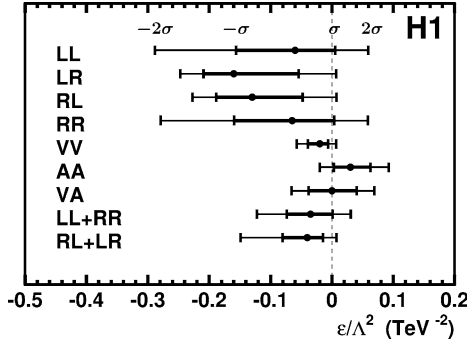
Fig. 2. Fit results on the parameters ϵ/Λ^2 of compositeness models using the combined e^+p and e^-p data. The inner and outer error bars represent one and two standard deviations, respectively, obtained by using experimental statistical and systematic errors.
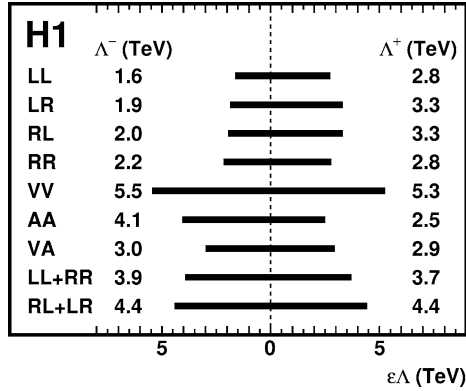

Fig. 3. Exclusion regions and lower limits (95% CL) on compositeness scale parameters $\Lambda^\pm$ for various chiral models obtained from the combined e^+p and e^-p data applying a frequentist method.

Fig. 3. The lower limits on compositeness scale parameters vary between 1.6 TeV and 5.5 TeV depending on the chiral structure. Choosing different parton distributions [9–11] changes the quoted limits typically by a few per cent, at most by 15%. The most restrictive bounds are observed for the VV model, where all chiral components contribute with the same sign. As an illustration, examples of fits to the e^-p and e^+p cross sections are shown in Fig. 4.

5. Leptoquarks

Leptoquarks couple to lepton–quark pairs and appear in extensions of the Standard Model which try to connect the lepton and quark sectors. They are colour triplet scalar or vector bosons, carrying lepton (L) and baryon (B) number and a fermion number $F = L + 3B$. Since $F = 2$ for e^-q and $F = 0$ for e^+q states, one expects different sensitivities to particular leptoquark types from electron and positron scattering. For high enough mass scales the leptoquark mass M_{LQ} and its coupling λ are related to the contact interaction coefficients via

$$\eta_{ab}^q = \epsilon_{ab}^q \frac{\lambda^2}{M_{LQ}^2}.$$

Within the model of [14] the production and decay modes are fixed and the relative contributions ϵ_{ab}^q have been calculated [15]. The notation, quantum numbers and couplings of the various leptoquarks are given in Table 3.

The analyses of the cross section measurements do not show an indication of a leptoquark signal.

Table 2
Lower limits (95% CL) on compositeness scale parameters $\Lambda^\pm$ for various chiral structures. Results are given for the present analysis of e^-p and e^+p data and for a combined analysis including e^+p data at $\sqrt{s} = 301$ GeV [2]

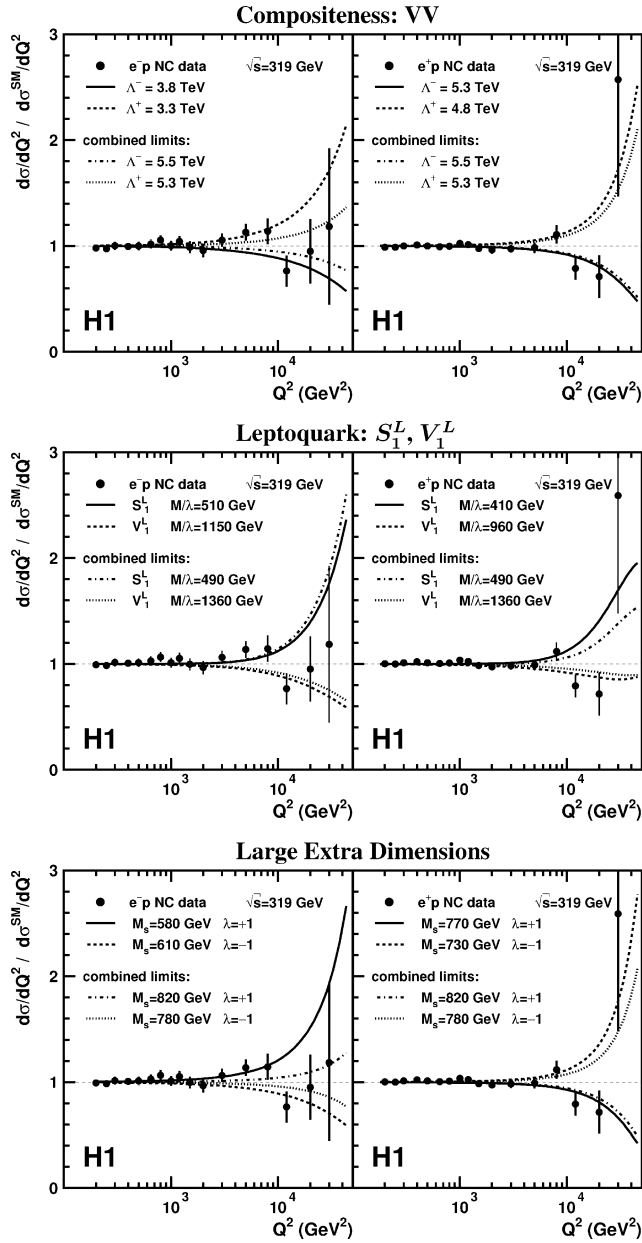| Coupling	e^-p (319 GeV)		e^+p (319 GeV)		all e^+p and e^-p	
	Λ^+ (TeV)	Λ^- (TeV)	Λ^+ (TeV)	Λ^- (TeV)	Λ^+ (TeV)	Λ^- (TeV)
LL	2.4	1.3	2.3	1.3	2.8	1.6
RR	2.4	1.4	2.4	1.3	2.8	2.2
LR	1.4	1.2	3.1	1.8	3.3	1.9
RL	1.4	1.2	3.1	1.9	3.3	2.0
VV	3.3	3.8	4.8	5.3	5.3	5.5
AA	3.2	1.6	2.3	3.7	2.5	4.1
VA	2.4	2.3	2.8	2.9	2.9	3.0
$LL + RR$	3.1	3.4	3.1	2.3	3.7	3.9
$RL + LR$	1.8	1.4	4.2	4.0	4.4	4.4

Fig. 4. NC cross section $d\sigma/dQ^2$ at $\sqrt{s} = 319$ GeV normalised to the Standard Model expectation. H1 e^-p and e^+p scattering data are compared with curves corresponding to 95% CL exclusion limits obtained from each data set and from the combined data for VV compositeness scales Λ^+ and Λ^- (top), couplings M/λ of leptoquarks S_1^L and V_1^L (center), gravitational scales M_S assuming positive ($\lambda = +1$) and negative ($\lambda = -1$) couplings (bottom). The errors represent only statistics and uncorrelated experimental systematics.

The results of fits for each type of leptoquark are interpreted in terms of limits on the ratio M_{LQ}/λ and are summarised in Table 3. In some cases, e.g., S_1^L and V_1^L, the e^-p data give more restrictive bounds than

e^+p scattering despite the lower integrated luminosity. This sensitivity is illustrated in Fig. 4, which shows possible contributions of the leptoquarks S_1^L and V_1^L to the e^-p and e^+p cross sections. The two leptoquarks

Table 3
Coupling coefficients η^q_{ab}, fermion number F and 95% CL lower limits on M_{LQ}/λ for scalar (S) and vector (V) leptoquarks. Results are given for the present analysis of $e^- p$ and $e^+ p$ data and for a combined analysis including $e^+ p$ data at $\sqrt{s} = 301$ GeV [2]. L and R denote the lepton chirality. The subscript $I = 0, 1/2, 1$ is the weak isospin. $\widetilde{S}$ and $\widetilde{V}$ differ by two units of hypercharge from S and V, respectively. Quantum numbers and helicities refer to $e^- q$ and $e^- \bar{q}$ states

LQ	$\eta^q_{ab} = \epsilon^q_{ab} \cdot (\lambda/M_{LQ})^2$		F	$e^- p$ (319 GeV)	$e^+ p$ (319 GeV)	all $e^+ p$ and $e^- p$
	ϵ^u_{ab}	ϵ^d_{ab}		M_{LQ}/λ (GeV)	M_{LQ}/λ (GeV)	M_{LQ}/λ (GeV)
S_0^L	$\epsilon^u_{LL} = +\frac{1}{2}$		2	530	610	710
S_0^R	$\epsilon^u_{RR} = +\frac{1}{2}$		2	480	560	640
$\widetilde{S}_0^R$		$\epsilon^d_{RR} = +\frac{1}{2}$	2	220	220	330
$S_{1/2}^L$	$\epsilon^u_{LR} = -\frac{1}{2}$		0	290	760	850
$S_{1/2}^R$	$\epsilon^u_{RL} = -\frac{1}{2}$	$\epsilon^d_{RL} = -\frac{1}{2}$	0	220	370	370
$\widetilde{S}_{1/2}^L$		$\epsilon^d_{LR} = -\frac{1}{2}$	0	200	410	430
S_1^L	$\epsilon^u_{LL} = +\frac{1}{2}$	$\epsilon^d_{LL} = +1$	2	510	410	490
V_0^L		$\epsilon^d_{LL} = -1$	0	480	660	730
V_0^R		$\epsilon^d_{RR} = -1$	0	420	550	580
$\widetilde{V}_0^R$	$\epsilon^u_{RR} = -1$		0	810	750	990
$V_{1/2}^L$		$\epsilon^d_{LR} = +1$	2	280	410	420
$V_{1/2}^R$	$\epsilon^u_{RL} = +1$	$\epsilon^d_{RL} = +1$	2	390	890	950
$\widetilde{V}_{1/2}^L$	$\epsilon^u_{LR} = +1$		2	400	970	1020
V_1^L	$\epsilon^u_{LL} = -2$	$\epsilon^d_{LL} = -1$	0	1150	960	1360

differ by their spin and couple with the same chiral structure but different strength and sign to u and d quarks. This emphasises the complementary role and importance of both electron and positron beams. The combined analyses of all $e^\pm p$ data further constrain the search for leptoquarks, reaching exclusion values of up to $M_{LQ}/\lambda = 1.4$ TeV. Note that upper bounds on the coupling strength λ can only be set for leptoquark masses exceeding the accessible centre of mass energy of HERA.

6. Squarks in R_p violating supersymmetry

In the most general formulation of supersymmetry there exist operators which couple a lepton-quark pair to a squark, the scalar superpartner of a quark. Such couplings violate R-parity (via lepton number violation), defined as $R_p = (-1)^{3B+L+2S}$ with S being the spin. Thus $R_p = +1$ for SM particles and $R_p = -1$ for superpartners. This interaction allows single squarks to be produced or exchanged in deep inelastic scattering [16] via

$$e^+ d_R \rightarrow \tilde{u}_L, \, \tilde{c}_L, \, \tilde{t}_L \quad \text{coupling } \lambda'_{1j1}, \tag{3}$$

$$e^+ \bar{u}_L \rightarrow \bar{\tilde{d}}_R, \, \bar{\tilde{s}}_R, \, \bar{\tilde{b}}_R \quad \text{coupling } \lambda'_{11k}. \tag{4}$$

The subscripts ijk of the coupling λ'_{ijk} describe the generation indices of the left-handed leptons, the left-handed quarks and the right-handed *down-type* quarks of the superfields, respectively.

The $e^+ q$ coupling of the left-handed *up-type* squark of reaction (3) is the same as that of the scalar leptoquark $\widetilde{S}_{1/2}^L$, and the coupling of the right-handed *down-type* squark of reaction (4) is the same as that of the scalar leptoquark S_0^L. Therefore, the formalism and results of the leptoquark analysis can be directly applied. Limits on the ratio $M_{\tilde{q}}/\lambda'$ for R_p violating squarks, assuming branching ratios $\mathcal{B}_{\tilde{q} \rightarrow eq} = 1$, are given in Table 4. Note that the squark generations cannot be distinguished in this analysis.

Table 4
Coefficients ϵ_{ab}^{q} and 95% CL lower limits on $M_{\tilde{q}}/\lambda'$ for R_p violating couplings to squarks. Results are given for the present analysis of $e^- p$ and $e^+ p$ data and for a combined analysis including $e^+ p$ data at $\sqrt{s} = 301$ GeV [2]

$\not{R}_p$ coupling	ϵ_{ab}^{q}	$e^- p$ (319 GeV) $M_{\tilde{q}}/\lambda'$ (GeV)	$e^+ p$ (319 GeV) $M_{\tilde{q}}/\lambda'$ (GeV)	all $e^+ p$ and $e^- p$ $M_{\tilde{q}}/\lambda'$ (GeV)
$\lambda'_{11k}\, e^+ \bar{u} \to \tilde{\bar{d}}^{(k)}$	$\epsilon_{LL}^{u} = +\frac{1}{2}$	530	610	710
$\lambda'_{1j1}\, e^+ d \to \tilde{u}^{(j)}$	$\epsilon_{LR}^{d} = -\frac{1}{2}$	200	410	430

7. Large extra dimensions

It has been suggested that the gravitational scale M_S in $(4 + n)$-dimensional string theory may be as low as the electroweak scale of order TeV [17]. The relation to the Planck scale $M_P \sim 10^{19}$ GeV and the size R of the n compactified extra dimensions is given by $M_P^2 \sim R^n M_S^{2+n}$. In some models with large extra dimensions the SM particles reside on a four-dimensional brane, while the spin 2 graviton propagates into the extra spatial dimensions and appears in the four-dimensional world as a tower of massive Kaluza–Klein states with a level spacing $\Delta m = 1/R$. The gravitons couple to the SM particles via the energy–momentum tensor with a tiny strength given by the inverse Planck scale. However, the summation over the enormous number of Kaluza–Klein states up to the ultraviolet cut-off scale, taken as M_S, leads to an effective contact-type interaction [18] with a coupling

$$\eta_G = \frac{\lambda}{M_S^4}.$$

The coefficient λ depends on details of the theory and is expected to be of order unity. However, by convention, one also allows for a negative coupling and thus sets $\lambda = \pm 1$. The scale dependence of gravitational effects is quite different from that of conventional contact interactions discussed in the previous sections.

The cross section formulae for virtual graviton exchange in DIS have been calculated in [1] using the conventions and formalism of [18]. The interference of the graviton with the photon and Z fields has opposite sign for electron and positron scattering, as illustrated in Fig. 4. Lower limits on the scale parameter M_S, derived from fits to the $d\sigma/dQ^2$ distributions including gravitational contributions, are summarised in Table 5. There is similar sensitivity to the effective gravitational scale for positive and negative interfer-

Table 5
Lower limits (95% CL) on the gravitational scale M_S assuming positive ($\lambda = +1$) and negative ($\lambda = -1$) coupling from the present analysis of $e^- p$ and $e^+ p$ data and from a combined analysis including $e^+ p$ data at $\sqrt{s} = 301$ GeV [2]

Coupling λ	$e^- p$ (319 GeV) M_S (TeV)	$e^+ p$ (319 GeV) M_S (TeV)	all $e^+ p$ and $e^- p$ M_S (TeV)
$+1$	0.58	0.77	0.82
-1	0.61	0.73	0.78

ence, resulting in lower limits of $M_S > 0.82$ TeV for $\lambda = +1$ and $M_S > 0.78$ TeV for $\lambda = -1$.

In other scenarios the gauge bosons γ and Z are also assumed to propagate into extra dimensions. This leads to analogous Kaluza–Klein states which couple to matter with electroweak strength and interfere with the ordinary gauge boson fields. In a specific model of $4 + 1 = 5$ dimensions [19] with compactification radius $R = 1/M_C$, the sums over the exchange of Kaluza–Klein gauge bosons essentially modify the photon propagator $1/Q^2 \to 1/Q^2 + \pi^2/(3M_C^2)$ and the Z propagator $1/(Q^2 + M_Z^2) \to 1/(Q^2 + M_Z^2) + \pi^2/(3M_C^2)$. A fit to the data yields $M_C > 1.0$ TeV as a lower limit at 95% CL for the compactification scale.

8. Form factors

A fermion substructure can also be formulated by assigning a finite size to the electroweak charge distributions. It is convenient to introduce electron and quark form factors $f(Q^2)$ which reduce the Standard Model cross section at high momentum transfer [20]:

$$f(Q^2) = 1 - \frac{\langle r^2 \rangle}{6} Q^2, \tag{5}$$

$$\frac{d\sigma}{dQ^2} = \frac{d\sigma^{SM}}{dQ^2} f_e^2(Q^2) f_q^2(Q^2). \tag{6}$$

Table 6

Upper limits (95% CL) on the quark radius R_q assuming point-like leptons ($f_e \equiv 1$) or common form factors ($f_e = f_q$) for the present analysis of $e^- p$ and $e^+ p$ data and from a combined analysis including $e^+ p$ data at $\sqrt{s} = 301$ GeV [2]

Form factor	$e^- p$ (319 GeV) R_q (10^{-18} m)	$e^+ p$ (319 GeV) R_q (10^{-18} m)	all $e^+ p$ and $e^- p$ R_q (10^{-18} m)
$f_e \equiv 1$	1.1	1.1	1.0
$f_e = f_q$	0.8	0.8	0.7

Fits to the data yield upper limits on the particle size $R = \sqrt{\langle r^2 \rangle}$, taken as the root of the mean squared radius of the electroweak charge distribution. Assuming a point-like electron, i.e., setting $f_e \equiv 1$, the radius of the light u and d quarks can be constrained to $R_q < 1.0 \times 10^{-18}$ m at 95% CL. If both electrons and quarks are assumed to have common form factors one obtains limits on fermion sizes of $R_{e,q} < 0.7 \times 10^{-18}$ m. The results of the analysis are given in Table 6.

9. Summary

Neutral current deep inelastic $e^- p$ and $e^+ p$ scattering cross section measurements are analysed to search for new phenomena mediated through $(\bar{e}e)(\bar{q}q)$ contact interactions. The data are well described by the Standard Model expectations. The use of electrons and positrons provides complementary information and a combined analysis based on an integrated luminosity of 117.2 pb^{-1} yields improved limits on scales of new physics. The present analysis supersedes previous results [1].

Lower limits at 95% CL on eq compositeness scale parameters $\Lambda^{\pm}$ are derived within a model independent analysis. They range between 1.6 and 5.5 TeV depending on the chiral structure. A study of virtual leptoquark exchange yields lower limits on the ratio M_{LQ}/λ between 0.3 and 1.4 TeV. Squarks in R-parity violating supersymmetry with masses satisfying $M_{\tilde{u}}/\lambda'_{1j1} < 0.43$ TeV and $M_{\tilde{d}}/\lambda'_{11k} < 0.71$ TeV can be excluded. Possible effects of low scale quantum gravity with gravitons propagating into extra spatial dimensions are searched for. Lower limits on the effective Planck scale M_S of 0.78–0.82 TeV are found. Allowing for Kaluza–Klein states of the SM gauge bosons results in a lower limit on the extra dimension

compactification scale $M_C > 1.0$ TeV. A form factor approach yields an upper limit on the size of light u and d quarks of $R_q < 1.0 \times 10^{-18}$ m assuming point-like electrons.

Appendix A. Setting limits

For the present analysis several methods have been studied to calculate limits and confidence levels and the final results quoted are based on the frequentist approach (see, for example, [21]). The χ^2 function of Eq. (1) is used as the quality measure of agreement between data and contact interaction models. It allows an easy implementation of systematic uncertainties. The other methods investigated differ in the definitions of the statistical error entering the total error $\Delta\hat{\sigma}_i$ in the χ^2 expression.

Taking the statistical errors of the experiment, one can test the compatibility of the data with a certain model hypothesis and determine the corresponding parameter, for example, $1/\Lambda^2$. Each data point contributes with a fixed weight $\Delta\hat{\sigma}_i^{-2}$ to the χ^2 function, independent of the model parameter. However, downward fluctuations with respect to the model predictions get a larger weight (smaller statistical error) than upward fluctuations (larger statistical error). This property may enforce asymmetric situations and errors, as is observed in the present data, see Fig. 2. If the fitted parameter is found to be not significantly different from zero, the result can be converted into limits at a given confidence level (CL). A convenient way is to take the values corresponding to a change of $\chi^2(1/\Lambda^{\pm 2}) - \chi^2_{SM} = \Delta\chi^2_{CL}$, for instance, $\Delta\chi^2_{95\%} = 3.84$ for a 95% CL limit. This method was used in the previous publication [1] and is illustrated for sev-
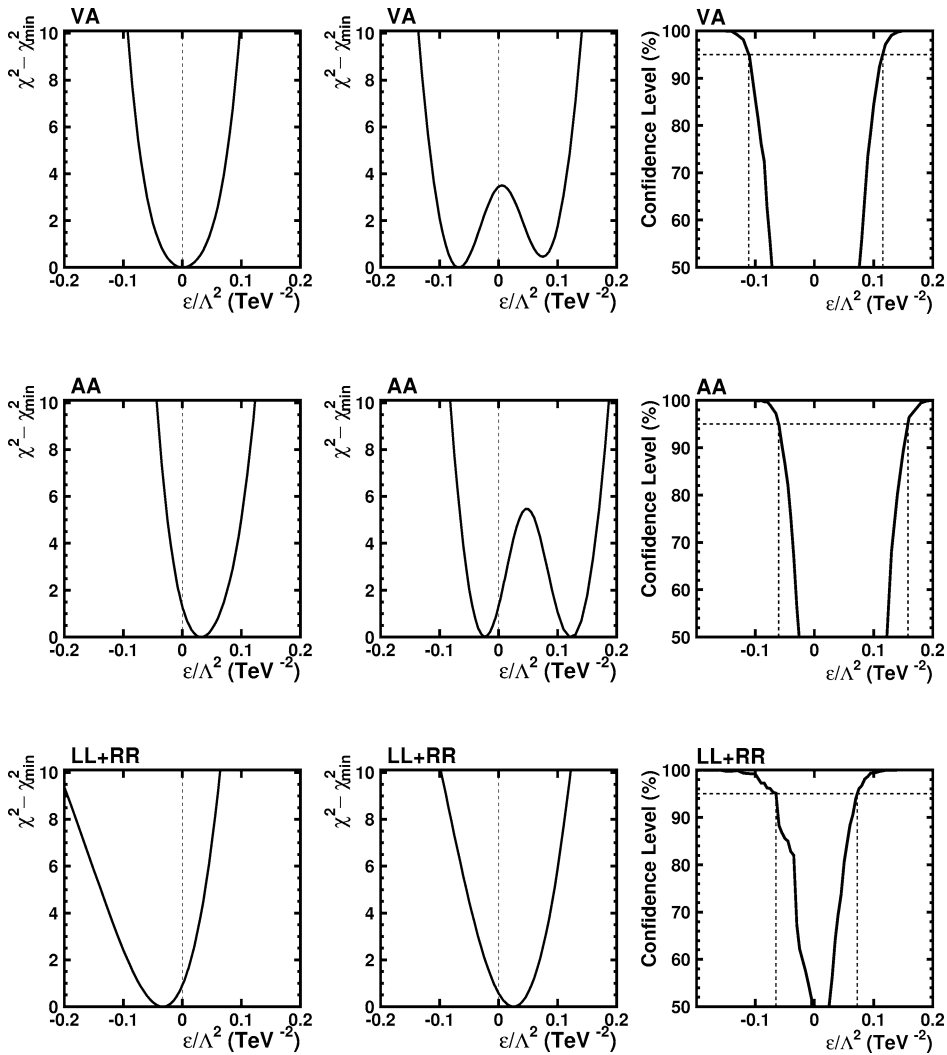
Fig. 5. Examples of different methods to calculate limits on the compositeness scale Λ for VA, AA and $LL + RR$ models obtained from combined fits including all data. Distributions of $\chi^2 - \chi^2_{\min}$ versus ϵ/Λ^2 using statistical errors from the experiment (left) and statistical errors from the prediction (center). Confidence level versus ϵ/Λ^2 from the frequentist method with dashed lines indicating the 95% CL limits for positive and negative interference (right). In all cases systematics are included.

eral compositeness models by the χ^2 distributions in Fig. 5. This simple and robust definition is certainly meaningful for parabolic curves, but the probabilistic interpretation becomes ambiguous if there are secondary minima or other structures.

An alternative possibility is to assume the validity of a certain CI model and to calculate the probability to observe the measured value for a given model parameter. Here the statistical error entering the χ^2

function is taken from the model prediction. This approach is completely equivalent to using the log-likelihood function, and it has been verified that both methods lead to the same results. Each data point gets a varying weight depending on the model parameter, but independent of fluctuations in the data. For the present data this leads to more symmetric situations and an unbiased evaluation. In general, the resulting χ^2 curves show a stronger sensitivity to details of

the CI model, e.g., interference patterns, as can be seen in Fig. 5. The widths of the distributions are often, but not always, wider than in the previous case. The problem to extract limits from these distributions persists.

The final limits presented here have been determined by applying a frequentist approach. Starting from a specific model with a scale parameter Λ_{true} the cross section $d\sigma/dQ^2$ is calculated and then smeared according to the statistical error given by the predicted number of events. Distortions due to all uncorrelated and correlated systematic uncertainties (except for the parton distributions) are included, assuming Gaussian behaviour of the errors. The Monte Carlo experiment is then analysed in the same way as the data, i.e., with statistical errors from the prediction and including all systematics, resulting in a fitted value Λ_{fit}. This procedure is repeated numerous times and the fit results are recorded in a probability distribution. The scale parameter is then varied and the 95% confidence lower limit Λ^+ (Λ^-) is defined as that value Λ_{true} where 95% of the Monte Carlo experiments produce values of Λ_{fit} which are larger (smaller) than the parameter Λ actually obtained from the data. Examples of CL distributions are shown in Fig. 5. For the present analysis the frequentist approach provides in general slightly weaker and more symmetric limits than the statistical method used previously [1].

References

[1] C. Adloff, et al., H1 Collaboration, Phys. Lett. B 479 (2000) 358, hep-ex/0003002.

[2] C. Adloff, et al., H1 Collaboration, Eur. Phys. J. C 13 (2000) 609, hep-ex/9908059.

[3] C. Adloff, et al., H1 Collaboration, Eur. Phys. J. C 19 (2001) 269, hep-ex/0012052.

[4] C. Adloff, et al., H1 Collaboration, hep-ex/0304003, DESY 03-038, Eur. Phys. J. C, submitted for publication.

[5] J. Breitweg, et al., ZEUS Collaboration, Eur. Phys. J. C 14 (2000) 239, hep-ex/9905039.

[6] R. Barate, et al., ALEPH Collaboration, Eur. Phys. J. C 12 (2000) 183, hep-ex/9904011;
P. Abreu, et al., DELPHI Collaboration, Eur. Phys. J. C 11 (1999) 383;
P. Abreu, et al., Phys. Lett. B 485 (2000) 45, hep-ex/0103025;
M. Acciarri, et al., L3 Collaboration, Phys. Lett. B 489 (2000) 81, hep-ex/0005028;
M. Acciarri, et al., Phys. Lett. B 470 (1999) 281, hep-ex/9910056;
G. Abbiendi, et al., OPAL Collaboration, Eur. Phys. J. C 13 (2000) 553, hep-ex/9908008.

[7] F. Abe, et al., CDF Collaboration, Phys. Rev. Lett. 79 (1997) 2192;
B. Abbott, et al., D0 Collaboration, Phys. Rev. Lett. 82 (1999) 4769, hep-ex/9812010.

[8] H.-L. Lai, et al., Eur. Phys. J. C 12 (2000) 375, hep-ph/0201195.

[9] J. Pumplin, et al., JHEP 0207 (2002) 012, hep-ph/0201195.

[10] A.D. Martin, R.G. Roberts, W.J. Stirling, R.S. Thorne, Eur. Phys. J. C 14 (2000) 133, hep-ph/9907231.

[11] M. Glück, E. Reya, A. Vogt, Z. Phys. C 67 (1995) 433.

[12] E. Eichten, K.D. Lane, M.E. Peskin, Phys. Rev. Lett. 50 (1983) 811;
R. Rückl, Phys. Lett. B 129 (1983) 363;
R. Rückl, Nucl. Phys. B 234 (1984) 91.

[13] P. Haberl, F. Schrempp, H.-U. Martyn, in: W. Buchmüller, G. Ingelman (Eds.), Proc. Workshop 'Physics at HERA', Vol. 2, DESY, Hamburg, 1991, p. 1133.

[14] W. Buchmüller, R. Rückl, D. Wyler, Phys. Lett. B 191 (1987) 422;
W. Buchmüller, R. Rückl, D. Wyler, Phys. Lett. B 448 (1999) 320, Erratum.

[15] J. Kalinowski, R. Rückl, H. Spiesberger, P.M. Zerwas, Z. Phys. C 74 (1997) 595, hep-ph/9703288.

[16] J. Butterworth, H. Dreiner, Nucl. Phys. B 397 (1993) 3, hep-ph/9211204.

[17] N. Arkani-Hamed, S. Dimopoulos, G.R. Dvali, Phys. Lett. B 429 (1998) 263, hep-ph/9803315;
N. Arkani-Hamed, S. Dimopoulos, G.R. Dvali, Phys. Rev. D 59 (1999) 08600, hep-ph/9807344.

[18] G.F. Giudice, R. Rattazzi, J.D. Wells, Nucl. Phys. B 544 (1999) 3, corrections in hep-ph/9811291.

[19] K. Cheung, G. Landsberg, Phys. Rev. D 65 (2002) 076003, hep-ph/0110346.

[20] G. Köpp, D. Schaile, M. Spira, P.M. Zerwas, Z. Phys. C 65 (1995) 545, hep-ph/9409457.

[21] D.E. Groom, et al., Particle Data Group, Eur. Phys. J. C 15 (2000) 1.